

North Atlantic Winter Climate Regimes: Spatial Asymmetry, Stationarity with Time, and Oceanic Forcing

CHRISTOPHE CASSOU

CERFACS-SUC, Climate Modelling and Global Change Team, Toulouse, France, and NCAR, Climate Global Dynamics Division, Boulder, Colorado

LAURENT TERRAY

CERFACS-SUC, Climate Modelling and Global Change Team, Toulouse, France

JAMES W. HURRELL AND CLARA DESER

NCAR, Climate Global Dynamics Division, Boulder, Colorado

(Manuscript received 25 October 2002, in final form 26 May 2003)

ABSTRACT

The observed low-frequency winter atmospheric variability of the North Atlantic–European region and its relationship with global surface oceanic conditions is investigated based on the climate and weather regimes paradigm.

Asymmetries between the two phases of the North Atlantic Oscillation (NAO) are found in the position of the Azores high and, to a weaker extent, the Icelandic low. There is a significant eastward displacement or expansion toward Europe for the NAO+ climate regime compared to the NAO– regime. This barotropic signal is found in different datasets and for two quasi-independent periods of record (1900–60 and 1950–2001); hence, it appears to be intrinsic to the NAO+ phase. Strong spatial similarities between weather and climate regimes suggest that the latter, representing long time scale variability, can be interpreted as the time-averaging signature of much shorter time scale processes. Model results from the ARPEGE atmospheric general circulation model are used to validate observed findings. They confirm in particular the eastward shift of the Atlantic centers of action for the NAO+ phase and strongly suggest a synoptic origin as it can be extracted from daily analyses. These results bring together present-day climate variability and scenario studies where such an NAO shift was suggested, as it is shown that the last three decades are clearly dominated by the occurrence of NAO+ regimes when concentrations of greenhouse gases are rapidly increasing. These findings highlight that the displacement of the North Atlantic centers of action should be treated as a dynamical property of the North Atlantic atmosphere and not as a mean longitudinal shift of climatological entities in response to anthropogenic forcings.

The nonstationarity with time of the atmospheric variability is documented. Late-century decades differ from early ones by the predominance of NAO climate regimes versus others. In such a context, comments on the relevance of the station-based NAO index is provided. Both tropical and extratropical sea surface temperature (SST) anomalies alter the frequency distribution of the North Atlantic regimes. Evidence is presented that the so-called ridge regime is preferably excited during La Niña events, while the NAO regimes are associated with the North Atlantic SST tripole. The ARPEGE model results indicate that the tropical branch of the SST tripole affects the NAO regimes occurrence. Warm tropical SST anomalies are more efficient at exciting NAO– regimes than cold anomalies are at forcing NAO+ regimes. The extratropical portion of the North Atlantic SST tripole also seems to play a significant role in the model, tending to counteract the dominant influence of the tropical Atlantic basin on NAO regimes.

1. Introduction

During the past few decades, there has been considerable effort devoted to obtaining a better understanding of natural climate variability over the North Atlantic–

European (NAE) sector on monthly to multidecadal time scales. The low-frequency extratropical atmosphere has been generally described in terms of space-stationary and time-fluctuating structures known as “teleconnection patterns” (Wallace and Gutzler 1981). Linear techniques such as one-point correlation, eigenmodes decomposition, etc., have been traditionally used to reveal the teleconnection patterns at various time scales (Blackmon et al. 1984). Viewed in a multidimensional phase space whose directions are defined by eigenvec-

Corresponding author address: Dr. Christophe Cassou, NCAR, Climate Modelling and Global Change Team, P.O. Box 3000, Boulder, CO 80307.
E-mail: cassou@ucar.edu

tors, the linear approach relies on the hypothesis that the climatological mean state is at the center of the phase space, the anomaly patterns being equally distributed along a given direction. However, there is no guarantee that preferred atmospheric circulation states come in pairs in which the spatial structure of the anomalies are the same, but of opposite polarity. Interest in this nonlinear interpretation of atmospheric variability has been growing, finding some applications within climate frameworks (Palmer 1999) as opposed to weather issues where this approach has been more commonly used.

The nonlinear paradigm is based on the identification of “attractors” that correspond to weather or climate regimes (Lorenz 1963) being defined as peaks in the probability density function of the climate phase space. A modification of the climate mean state or low-frequency climate variability is then interpreted as a change in the amplitude of these peaks or in the preferred transitions between them (e.g., Robertson et al. 2000) leading to changes in their frequency of occurrence rather than changes in the modes themselves. Few statistical methods are able to take into consideration both asymmetry and time scale interactions in the determination of variability patterns. Cluster analysis is one of them and will be the central tool of our study. It is a multivariate statistical technique based on the property of a collection of events to group together into a small number of representative states (or regimes) according to a given criterion of similarity. Either raw daily maps (Michelangeli et al. 1995) or 10-day low-pass-filtered ones (e.g., Kimoto and Ghil 1993) are traditionally classified. Some recent studies have, however, focused attention on monthly means and have linked the month-to-month atmospheric variability to longer low-frequency time scales. For example, Corti et al. (1999) find that the recent temperature trend over the Northern Hemisphere is related to the preferred occurrence of the so-called cold ocean warm land monthly regime. Monahan et al. (2001), based on a generalized empirical orthogonal function (EOF) technique that does not constrain modes to be linear, show that the regimes related to the so-called Arctic Oscillation (Thompson and Wallace 1998) are favored in a warmer climate.

Observed monthly means are first used in the present study to investigate the signature of the NAE interannual variability in terms of climate regimes. Monthly means cannot be interpreted as quasi-stationary regimes but should rather be considered as the time average of rapidly fluctuating entities, known as weather regimes (Vautard 1990), with a typical 8–10-day e -folding time scale (Feldstein 2000). Therefore, our goal is not to conduct a dynamical study of the atmospheric fluctuations but to extract the signature of potential ocean forcings that may affect the excitation of weather regimes and have a clearer signature when averaged over a month. Indeed time averaging is beneficial as it increases the signal-to-noise ratio in the data. On the other

hand, it reduces the sampling size and may affect the robustness of statistical results.

The clustering methods used in this study are described in section 2. The NAE climate regimes are presented in section 3 over two different periods and from two different datasets. Discussion about their spatial asymmetry as well as their stationarity over the twentieth century are reported. Their links to oceanic conditions are described in section 4. The Action de Recherche Petit Echelle Grande Echelle (ARPEGE) atmospheric global circulation model is used to further investigate the nature of the oceanic forcing on the North Atlantic atmosphere. Similarities between weather and climate regimes are discussed to illustrate the hypothesis that oceanic forcings affect the frequency distribution of the weather regimes, the climate regimes occurrence being explained by the temporal integration of the latter. In this section emphasis is also put on the respective impact of tropical versus extratropical oceanic conditions on simulated weather regimes. A summary and perspective are given in section 5.

2. Classification techniques

Clustering algorithms are usually divided into two types of schemes, namely, hierarchical and partitional methods (Anderberg 1973). The former organizes states into nested sequences of clusters forming a growing aggregation tree, the latter iteratively performs the classification from randomly predefined initial centroids according to a pregiven number k of clusters. As pointed out in Alhamed et al. (2002) and due to the sampling size, it is central to test the robustness of the cluster solution with different types of algorithms since different schemes and different similarity criteria can lead to different conclusions. In this study, results are presented either for the Ward's hierarchical technique (Ward 1963; Cheng and Wallace 1993) or for the k -means partitional scheme (Michelangeli et al. 1995), but it has been verified for all the decompositions, that the two clustering approaches give similar regimes for the same number of clusters used.

At each step n ($n = 1, N - 1 - k$) of clustering, N standing for the total number of samples and k for the final number of clusters retained, the Ward's scheme retains among all possible aggregations the one that minimizes the so-called intercluster inertia. The latter represents the sum over $N - n$ clusters of the dispersion from their respective centroids (Martineu et al. 1999). For the k -means algorithm, the classification is performed on the first 10 principal components of the anomalous maps by minimizing the quadratic distance to a number of arbitrary predetermined k centroids. For this specific number, the partition is performed 100 times with a different set of arbitrary determined centroids and the classification retained is the one that correlates best with the 99 others. This correlation value is used to compute the so-called classificability index

that tests, for each decomposition in k regimes, its significance against an artificial red-noise dataset with the same statistical characteristics as the physical and original one. The so-called optimal k number is given by the highest significant correlation value and can be interpreted as the one obtained for the most robust and physical classification. Besides cross-validation consideration, the Ward and the k -means algorithms are thus complementary as the latter provided the optimal k number of clusters to be retained whereas the final number of regimes to keep at the end of the iterative process remains somewhat subjective for hierarchical schemes.

3. Climate regimes over the North Atlantic–European region

Cluster analyses are first applied to monthly sea level pressure (SLP) means from the National Centers for Environmental Prediction–National Center for Atmospheric Research (NCEP–NCAR) reanalysis (Kalnay et al. 1996) for 1950–2001 (hereafter NCEP). The statistical decomposition is performed for individual winter months [December–January–February (DJF)] over the NAE domain (20° – 80° N, 80° W– 30° E), where each month is considered an individual realization of the atmospheric states. The clustering partition yields the optimal $k = 4$ number of significant winter climate regimes subsequently represented by the cluster centroid. The latter includes all the classified months averaged for a given cluster and it has been verified that limited averaging to the closest states around the cluster centroid does not significantly affect the regimes spatial characteristics but enhances their spatial significance (not shown). The first two clusters (Figs. 1a,b) capture the negative and the positive phases of the North Atlantic Oscillation (NAO) and are characterized by a zonally elongated meridional pressure dipole between the Icelandic low and the Azores high. The third cluster (Fig. 1c) displays a strong anticyclonic ridge (RDG) off western Europe almost covering the entire basin. It is reminiscent of the positive phase of the east Atlantic (EA) teleconnection pattern (Wallace and Gutzler 1981) which features the northward extension of the Azores high. The fourth cluster (Fig. 1d) exhibits a zonal pressure dipole between Greenland and Scandinavia (GS) with a clear southeastward extension of low pressure anomalies toward the Iberian Peninsula. The GS cluster has been revealed as the third or fourth EOF mode over the NAE domain (Davies et al. 1997), and it is reminiscent of the Eurasian mode of Barnston and Livezey (1987), although unlike EOF modes the regime patterns are sign definite.

The time history of occurrence of the NAO regimes (Fig. 1e) shows strong interannual variability. Negative NAO (NAO $-$) phases are predominant in the 1950s and 1960s while positive NAO (NAO $+$) regimes are clearly excited over the last two decades excluding NAO $-$ states (except for the winters of 1996 and 2001). This

is consistent with the observed upward NAO index trend as described in Hurrell (1995). Although less striking, the RDG pattern seems to be favored at the beginning of the 1950s and over the 1965–76 period while no clear low-frequency changes characterize the GS seesaw regime (Fig. 1f). Note that GS occurrence generally corresponds to extreme cold outbreaks in Europe (Walsh et al. 2001) and is indicative of blocking conditions. There is an overall good agreement between the occurrence of the NAO regimes and the DJF-averaged NAO indices either calculated from station-based data (Hurrell and van Loon 1997) or derived from EOF decomposition (Fig. 1e). A careful year-to-year inspection reveals, however, some discrepancy. This is particularly striking when the NAO regimes are not dominant, yet the traditional NAO indices can have large values. As RDG mostly projects onto the NAO $+$ cluster, its predominance over the winter season may lead to significant positive NAO indices even if the NAO regime is not prevalent. This is the case at the beginning of the 1950s and for some isolated years such as 1981, 1994, and 1999. EOF analyses seem to be more adept at accounting for spatial coherence of the variability. They therefore capture the regime occurrence, but they should not be limited to the first leading mode in order to depict the full range of the NAE variability. Even if the NAO captures about 50% of the variance over the 1950–2001 period, EOF2 and EOF3 appear to be very important. It is important to mention that linearly or quadratically detrending the data does not significantly change the shape of the regimes or their temporal distribution.

The robustness of the classification has been verified by applying the same algorithm to an independent and longer SLP dataset updated from Trenberth and Paolino (1980, hereafter TP–NCAR). They combined several SLP station-based measurements from different sources from 1899 to present to form a $5^{\circ} \times 5^{\circ}$ latitude–longitude gridded dataset treated with several methods to correct errors and trends. The minimum pointwise spatial correlation between TP–NCAR regimes computed over 1950–2000 and those presented in Fig. 1 for NCEP is 0.81 (not shown). Figures 2a–2d present the four climate regimes computed from the TP–NCAR dataset but over the 1900–60 winters. For confirmation of the stability in the cluster decomposition, we have decided to keep in common one decade for the regime extraction. The decomposition over the overlapped period between NCEP and TP–NCAR leads to the same partition for 28 months out of 33 (Figs. 2e,f). The spatial characteristics of the four regimes appear to be independent of the period and dataset. The only significant difference with NCEP clusters is found for GS. The anomalous high pressure over Scandinavia is diminished and the Greenland low pressure anomalies are reinforced and displaced southeastward toward Ireland. The TP–NCAR GS regime tends to be a more symmetrical image of RDG compared to NCEP, and it exhibits a clear wavy structure.

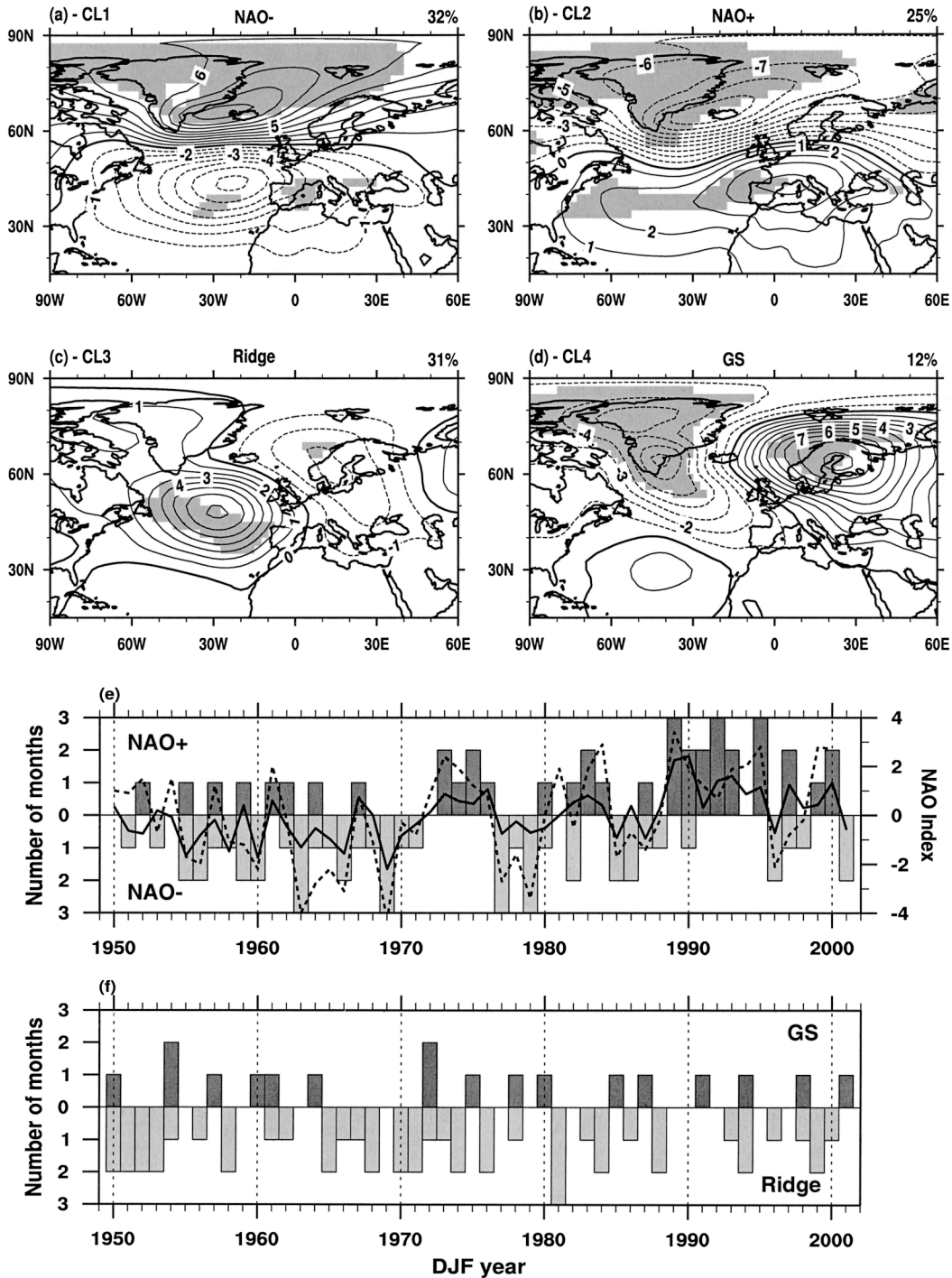


FIG. 1. (a), (b), (c), (d) 1949–2001 DJF mean SLP regimes (hPa) over the North Atlantic sector from NCEP reanalysis. Shaded areas exceed the 95% confidence level using T and F statistics. The percentage at the top right of each panel gives the global population of a given cluster over the whole period. Contour interval is 1 hPa. (e), (f) Time history of the occurrence for the NAO and the RDG–GS regimes, respectively. The vertical bars indicate the number of months relative to each winter where the given regime is present. Solid line stands for the standardized expansion coefficient of the leading DJF SLP EOF. The dashed line is the NAO index based on Hurrell and van Loon (1997). Note that because only one EOF2 and EOF3 phase is represented by the RDG and GS regimes, their associated time series are not shown in (f).

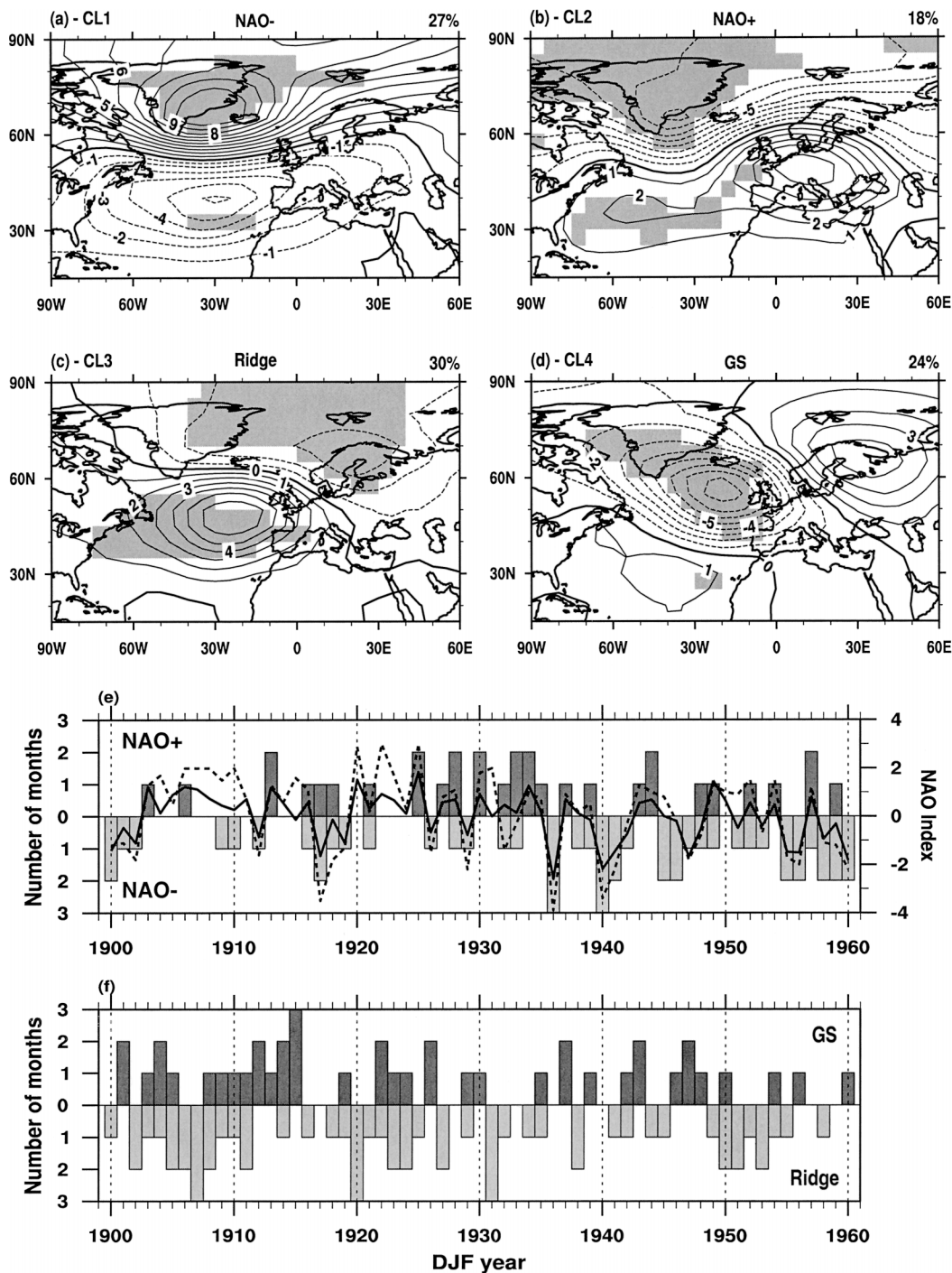


FIG. 2. Same as Fig. 1 but for the 1900–60 period and TP–NCAR dataset.

Interestingly, the nonlinear approach reveals some important spatial asymmetries between the phases of the NAO. The main difference between the two NAO regimes is in the position of the Azores high. The latter is eastward shifted by about 30° of longitude for the NAO+ case compared to the NAO- case. The Icelandic low center is more symmetric, but the low tends to

extend more northeastward toward Spitzberg for the NAO+ case (see also van Loon and Madden 1983). The general eastward shift of the centers of action of the NAO+ regime is not dependent on the time window considered (Figs. 1 and 2). This property has strong implications with respect to conclusions from climate scenario studies. Eastward displacements of the NAO

centers are seen in some scenario model experiments in which enhanced greenhouse gas concentrations are prescribed. These have been attributed to the mean climate drift due to anthropogenic external forcings (Ulbrich and Christoph 1999). Our results seem to indicate, however, that the northeastward shift of the centers of action may be better understood in terms of more frequent NAO+ regimes instead of simple static shifts of the Atlantic pressure centers. Such a conclusion is consistent with the tendency toward higher NAO index values simulated in most scenario studies (Gillet et al. 2003). Our interpretation is that the longitudinal apparent shift is an *indirect* consequence of excited NAO+ regimes that are *intrinsically* eastward displaced. It is interesting that the Météo-France model scenarios, which do not display a significant shift of the Atlantic centers of action, do not exhibit any trend toward positive NAO values (Drévilion 2002). Indications of a longitudinal shift for the NAO centers are found in observations as well, in Hilmer and Jung (2000). Their findings are based on the difference between two decadal periods (1958–77/1978–97) of winter SLP data regressed onto an ice volume export index through the Fram Strait. Our results go beyond their linear and epoch description however. Evidence of displacement appears more clearly when a dynamical nonlinear approach is applied and thus can be interpreted as the result of NAO+ regime dominance over the past 30 years.

The weak modification of the clusters over the century is consistent with the hypothesis that the centroids of the regimes are phase space regions of relative stability, being mostly linked to the quasi-daily atmospheric variability, but their excitation is subject to interannual to decadal changes. Note, for instance, that the NAO regimes (combined positive and negative phases) represent only 45% of the total sample over 1900–60 compared to 57% over the second part of the century. Figures 2e,f highlight that NAO dynamics are almost completely nonexistent over the 1900–25 period during which RDG and GS regimes were more dominant. For these two decades, the strongly positive traditional NAO indices may therefore be artificial and misleading. Results from this study are complementary to the ones presented in van Loon and Madden (1983). They show that the SLP variance is far from stationary and is affected by both the length and the time period considered. They highlight the singular behavior of the early twentieth century variability with a significant displacement of the maximum SLP variance from the Irminger Sea to Ireland (see their Figs. 1 and 3). The present study explains this shift as the excitation of RDG–GS regimes over this period. Such a conclusion can be partially assessed within the linear paradigm by comparing, as a function of time, values of explained variance for the two leading SLP EOF modes over the same domain. The NAO mode (52% of explained variance) clearly dominates the EA mode (17%) over the past 50 years

whereas they have almost the same weight (32% versus 28%) over 1900–25.

Several studies have emphasized that the short time scale dynamics of the NAO arises from the driving of synoptic-scale eddies, which is most prominent in the upper troposphere (e.g., Hoskins et al. 1983). To illustrate this hypothesis and to further confirm that the SLP decomposition presented so far is robust, Ward's algorithm is applied to the geopotential height field at 500 hPa (Z500) from NCEP. The cluster decomposition is performed over the same NAE domain and over the 1950–2001 period. The four Z500 regimes (Fig. 3) are very similar to their SLP counterparts and clearly illustrate the equivalent barotropic characteristics of the atmospheric patterns. Although structures are slightly displaced westward, the spatial asymmetry related to the NAO phase is still evident. Note that the Icelandic low displacement is enhanced for Z500. The wavy shape of the RDG regime is better extracted as well as for the GS regime, although the Scandinavian core has lost some significance. The temporal distribution of the four Z500 regimes is similar to the SLP classifications. NAO– and RDG regimes dominate, and 78% of the months are similarly classified among the four states in the SLP and Z500 cluster decompositions.

4. Sea surface temperature links

As mentioned earlier, the stability of the atmospheric regime centroids over time suggests that their existence is set by stationary and transient wave activity. Their excitation and associated transitions are mainly controlled by internal atmospheric processes, but external atmospheric forcings are expected to influence the frequency of transition into one weather regime or another, leading to changes in the climate regime occurrence. The latter could therefore be considered as the atmospheric time-averaged response of that particular time-averaged forcing (Feldstein 2000). In the rest of the paper, our goal will be to investigate the potential role of ocean anomalies in preferentially exciting the four natural atmospheric regimes extracted above. Results will be presented for both observations and model experiments.

a. Observations

The time history of the occurrence of the four NCEP regimes is used to build SST composites (Reynolds and Smith 1995). The events or years selected for the composite construction are those for which a given regime is dominant for at least two months out of three for a given winter (but only one month out of three for GS due to its weak occurrence over the 1950–2001 period). Due to the importance of the internal extratropical atmospheric variability, this two-month restriction reduces the likelihood that a regime can simply occur by chance without oceanic forcings.

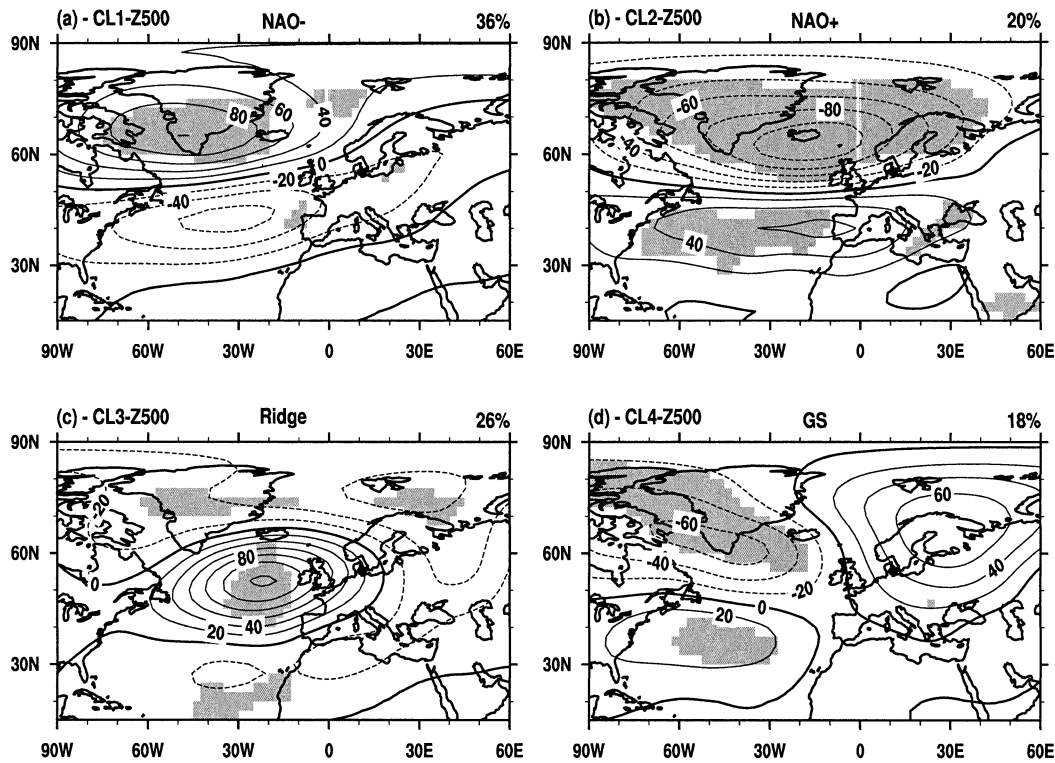


FIG. 3. Same as Figs. 1a–d but for Z500 from NCEP reanalysis.

The local Atlantic SST patterns first appear to be consistent with the atmospheric forcing of the ocean. The simultaneous winter SST anomaly patterns related to the NAO regimes display rather symmetrical features strongly projecting onto the North Atlantic tripole (Figs. 4a,b). Weak, insignificant equatorial warming occurs in the Pacific associated with the NAO+ regime. The RDG regime mainly captures a La Niña signal concomitant with a positive SST lobe off Newfoundland and cold subtropical North Atlantic anomalies (Fig. 4c). The GS regime is linked to weak cooling off Newfoundland and significant warming in the Norwegian Sea (Fig. 4d). Detrending the SST data does not change the composites, except for the NAO+ case for which the strength of the North Atlantic tripole is slightly weaker and the equatorial Pacific warming completely disappears. Note the asymmetries in the spatial structure of the SST tripole, especially its tropical branch. Maximum warming occurs off the Sahara coast in relation with NAO– regimes while the strongest cooling is located north of the South American continent for the NAO+ case. Such a discrepancy is consistent with the atmospheric spatial asymmetry between NAO phases and its forcing signature on the surface ocean. It is worth noting that the spatial displacements for both the NAO and SST modes can be indirectly found by compositing fields based on their respective expansion coefficients given by EOF techniques (not shown).

Simultaneous relationships do not give any infor-

mation on the possible feedback of the ocean on the atmospheric variability especially at midlatitudes. For this purpose, atmospheric models forced by observed oceanic conditions varying with time or by prescribed SST anomaly patterns are needed. In such a context, the ENSO impact onto the simulated North Atlantic dynamics has been recently investigated. Cassou and Terray (2001), for instance, show that the mean DJF ENSO signature simulated in the ARPEGE model (also found using signal-to-noise statistical techniques in different models; e.g., Venzke et al. 1999) projects well onto the RDG regime (see their Fig. 8). We have verified that it corresponds in fact to the averaged preferred excitation of the RDG regime in the model, which seems to be linked in that case to the Pacific–North America (PNA) arching pattern extending toward the western Atlantic. Note that the asymmetry between the ENSO phases (predominant La Niña influence on European climate compared to El Niño) appears to be consistent with numerous studies such as Chen (1982), Halpert and Ropelewski (1992), and Hannachi (2001) among others. To further test its relevance, we projected the raw SLP monthly maps onto RDG and took the -1 std dev threshold of the normalized time series to rebuild SST composites. No clear El Niño signature appeared in that case (not shown) reinforcing our confidence in the asymmetrical RDG–La Niña relationship. Differentiating between winter months, the Pacific–RDG connection appears to be strongest for December and dimin-

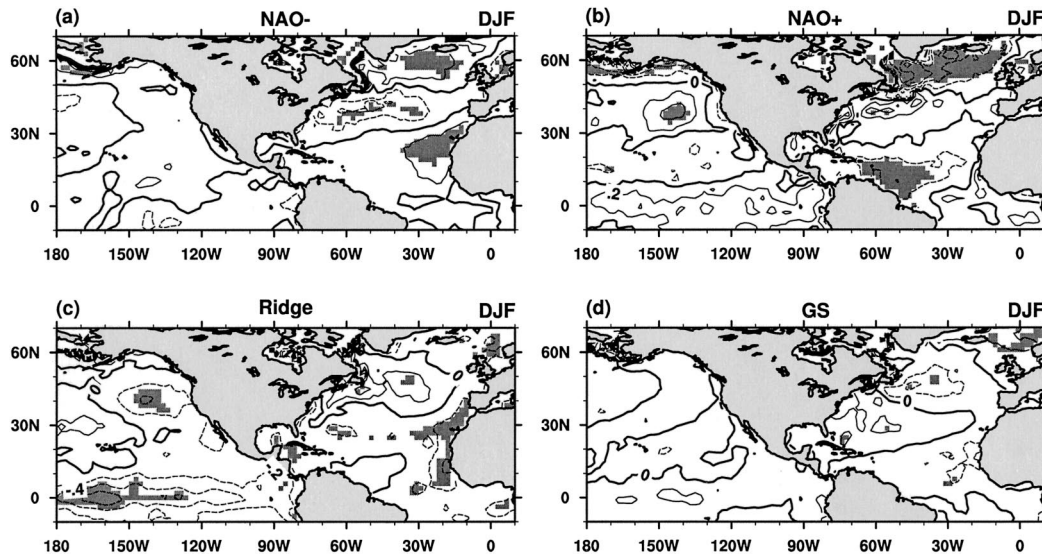


FIG. 4. Simultaneous DJF NCEP SST composites ($^{\circ}\text{C}$) related to the four NAE regimes. The events selected for the composite construction correspond to the year where the regime is dominant. SST monthly means corresponding to the particular months of these years where the regime is excited are averaged, the number of freedom of the composite being set to its most restrictive value given by the number of included years thus taking into account the month-to-month persistence of the SST. Shaded areas exceed the 95% confidence level using T and F statistics. Contour interval is 0.2°C .

ishes thereafter. This is consistent with the seasonal cycle of the equatorial SST variance in the Pacific yielding a minimum at early spring (Yu and McPhaden 1999). The potential role of the concomitant North Atlantic anomalies off Newfoundland on RDG is also reported in Peng and Fyfe (1996) and Watanabe and Kimoto (2000) from models. A quasi-barotropic response downstream of the SST anomaly center is described in these studies.

No clear indication of potential oceanic forcing upon GS is hypothesized. Further support for a primarily atmospheric forcing can be seen when a lag is introduced in the composite construction. Previous SST conditions do not exhibit any coherent basin-scale pattern while the following month SST composite shows a clear reinforcement of the DJF oceanic anomalies.

Regarding the NAO regimes, model results have suggested the forcing role of the North Atlantic SST tripole and especially the tropical part (Sutton et al. 2001). Terray and Cassou (2002) have shown in particular that the North Atlantic tropical basin affects the occurrence of the NAO climate regimes via the alteration of the Hadley cell and related modification of stationary and transient waves activity. They also comment on the spatial asymmetry of the related tropical SST patterns.

To confirm the leading role of the North Atlantic tripole and to better illustrate that the long time scale atmospheric variability described in the previous section from the climate regime approach represents the time-averaging of much shorter synoptic time scale processes, results are now presented from integrations of the AR-

PEGE AGCM where anomalous SST patterns have been introduced in the boundary conditions.

b. North Atlantic tripole forcing on atmospheric regimes

1) EXPERIMENTAL DESIGN

The Météo-France ARPEGE AGCM is derived from the Integrated Forecast System model developed and maintained by the European Centre for Medium-Range Weather Forecasts (ECMWF) and is described in Déqué et al. (1994). The present version uses a T63 triangular horizontal truncation. Diabatic fluxes and nonlinear terms are calculated on a Gaussian grid of about $2.8^{\circ} \times 2.8^{\circ}$ latitude–longitude. The vertical resolution is discretized over 31 levels (20 levels in the troposphere) using a progressive vertical hybrid coordinate extending from the ground up to about 34 km (7.5 hPa). The reader is invited to refer to Cassou and Terray (2001) for a detailed description of the model physics package and for its performance.

Six 30-yr model simulations have been carried out forced by three different anomalous oceanic patterns (Fig. 5) and their opposite in sign. The SST anomalies correspond to the oceanic conditions or “optimal forcing pattern” generating the most detectable atmospheric response after ENSO (Terray and Cassou 2002) over the NAE region in the ARPEGE model using maximizing signal-to-noise techniques (Allen and Smith 1997). Values have been scaled to reach about $\pm 1^{\circ}\text{C}$ off Africa and Newfoundland. The prescribed pattern bears a

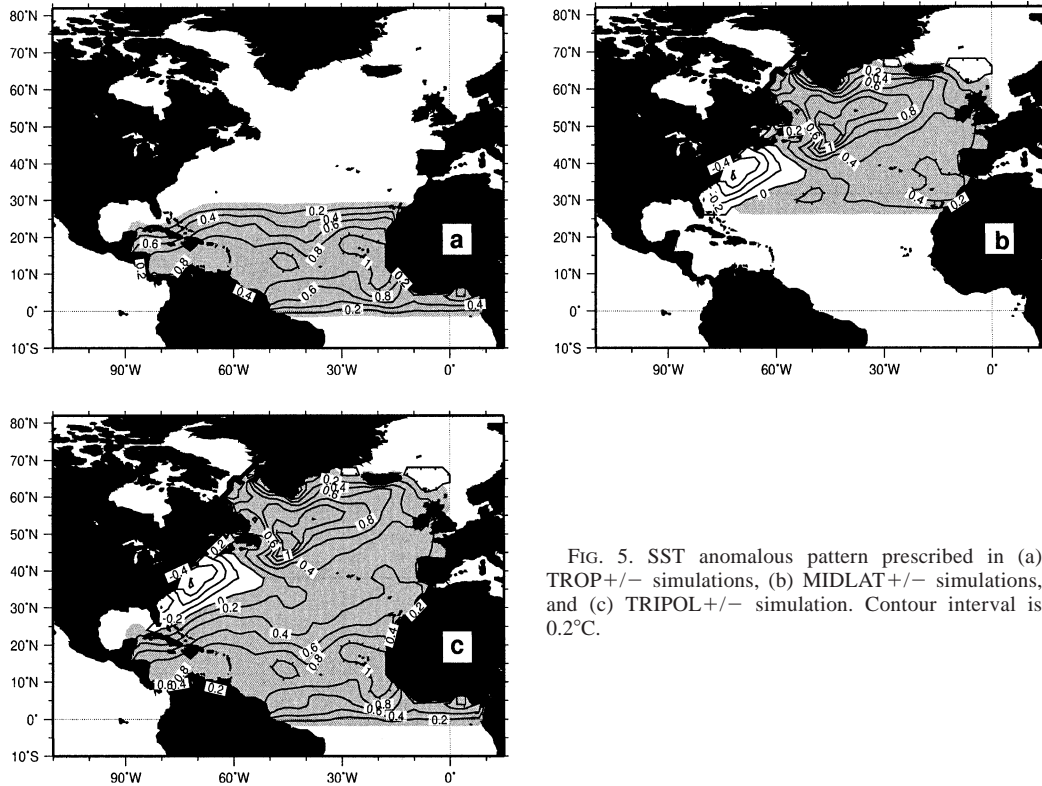


FIG. 5. SST anomalous pattern prescribed in (a) TROP+/- simulations, (b) MIDLAT+/- simulations, and (c) TRIPOL+/- simulation. Contour interval is 0.2°C.

strong similarity to the North Atlantic tripole previously extracted by composites and linked to the NAO regimes. Based on this resemblance, the choice has been made to specify the optimal pattern instead of the composite SST field in order to maximize the oceanic forcing on the atmosphere while staying close enough to the observed signals. It has been shown indeed that details in prescribed anomalous SST patterns can be important in shaping atmospheric model responses as the latter are often based on spatial resonance between imposed boundary conditions and simulated mean background flow (Peng and Whitaker 1999). Biases in the latter could therefore overcome the real role of the observed SST pattern as opposed to the optimal SST structure where those biases are indirectly taken into account. The drawback of this choice relies on the linearity constraint of the optimal filtering method. Therefore, the asymmetries of the oceanic composites described in the previous section and their potential impact on the atmosphere cannot be analyzed in the following simulation setup.

In the first set of experiments, the anomalous SST pattern is restricted to the tropical North Atlantic (0°–30°N; Fig. 5a) and two simulations have been performed with the positive (TROP+) and negative (TROP–) versions of the SST anomaly. In the second set of experiments, the anomalous SST pattern is restricted to the extratropical North Atlantic (above 30° of latitude; Fig. 5b) and similarly two simulations (MIDLAT+ and

MIDLAT–) are conducted. Finally, the third type of experiment combines the tropical and extratropical anomalous oceanic conditions (Fig. 5c) and will be referred to as TRIPOL+ and TRIPOL–. Anomalous oceanic patterns are applied from December to May.

The oceanic forcing is investigated from cluster analyses using the *k*-means algorithm applied on raw *daily* data of SLP from the model. All the six combined experiments are concatenated together with a 30-yr dataset (for consistency with the duration of the sensitivity experiments) from a 200-yr long control experiment where the seasonal cycle of the SST is repeated without anomaly. The partitioning has been done on the NAE domain and only winter days are selected. A total of 18 900 maps (7 experiments \times 90 days \times 30 yr) are thus classified and we have verified that the *weather* regimes are robust by subsampling and by performing the decomposition from the control run of the model only. The ARPEGE climate regimes are reported in Terray and Cassou (2002).

2) WEATHER–CLIMATE REGIME RELATIONSHIP

Four weather regimes have been extracted from ARPEGE. The first two regimes capture the positive and negative phase of the NAO (Figs. 6a,b). The third and fourth (Figs. 6c,d) are rather symmetrical with a strong SLP anomaly over the North Sea and will be respectively referred to as the northeast (NE) high and low.

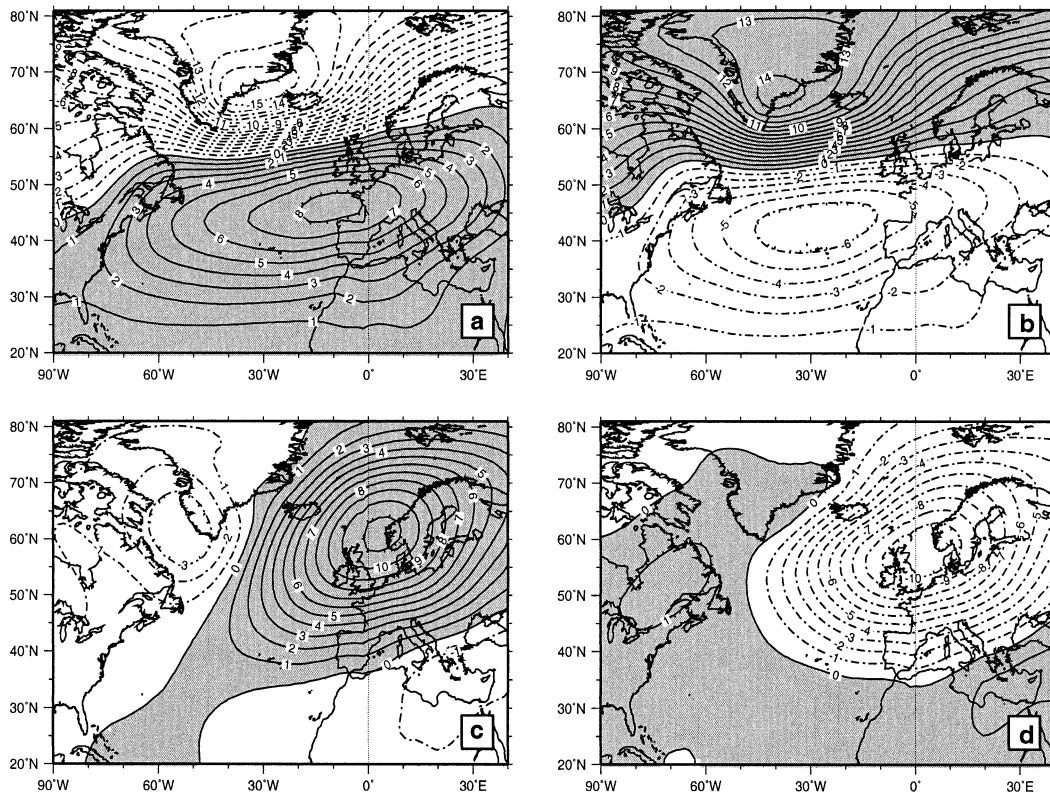


FIG. 6. SLP centroids of daily weather regimes (hPa) from ARPEGE experiments: (a) NAO+, (b) NAO-, (c) NE high, and (d) NE low. Contour interval is 1 hPa.

We have verified that the k -means cluster decomposition applied on NCEP winter daily data gives very similar results (Fig. 7). The minimum spatial correlation between NCEP and ARPEGE weather regimes is 0.83 and is obtained for NAO+ over 1950–2001.

The simulated and observed NAO weather regimes project remarkably well on the observed NAO climate regimes. Particularly striking is the eastward shift of the Azores high for NAO+ compared to NAO- that the model is able to represent, although less pronounced than for NCEP. This again indicates that the NAO climate regimes are the time-averaged signature of NAO-type quasi-daily fluctuations and that the displacement of the Azores high is a property of the positive NAO phase. The NE high is indicative of regional blocking. Daily composites on surface continental temperature and precipitation based on the days occupied by the NE high reveal very cold and dry conditions in central and eastern Europe (Cassou 2001). For the NE low, warm and very wet conditions dominate western and central Europe. The NE-high weather regime is reminiscent of the GS climate regime and would suggest that the latter also represents the time integration of shorter entities. Note though that the Greenland core is considerably reduced compared to the Scandinavian one for the daily case. We have verified that the occurrence of the NCEP NE high is maximum for months where the GS climate

regime is excited. By contrast, the RDG climate regime does not seem to have its reciprocal weather regime; however, the latter appears when the decomposition domain is limited to 0° of longitude instead of 30°E , thus excluding the NE-high/NE-low weight over Europe (not shown). The discrepancy between RDG weather and climate regimes decomposition could thus be explained by the statistical sensitivity to the region selected for clustering. It can also be partly explained by the persistence of the RDG weather regime. The latter can be rarely excited in total but be persistent when occurring. Persistence is not a criterion for the k -means clustering while it is indirectly taken into account in monthly means.

3) OCEAN IMPACT ON THE FREQUENCY DISTRIBUTION OF THE WEATHER REGIMES

Changes in the frequency of occurrence for the four weather regimes as a function of oceanic anomalies are now presented (Fig. 8). Contrasting TROP+ and TROP- shows that the tropical North Atlantic Ocean has an influence on the excitation of the NAO regimes. The NAO- (NAO+) regime is favored by about 6% (3%) in warm (cold) conditions, these differences in terms of percentage of occurrence being significant (6% represents a 1134-day difference) as tested in Robertson

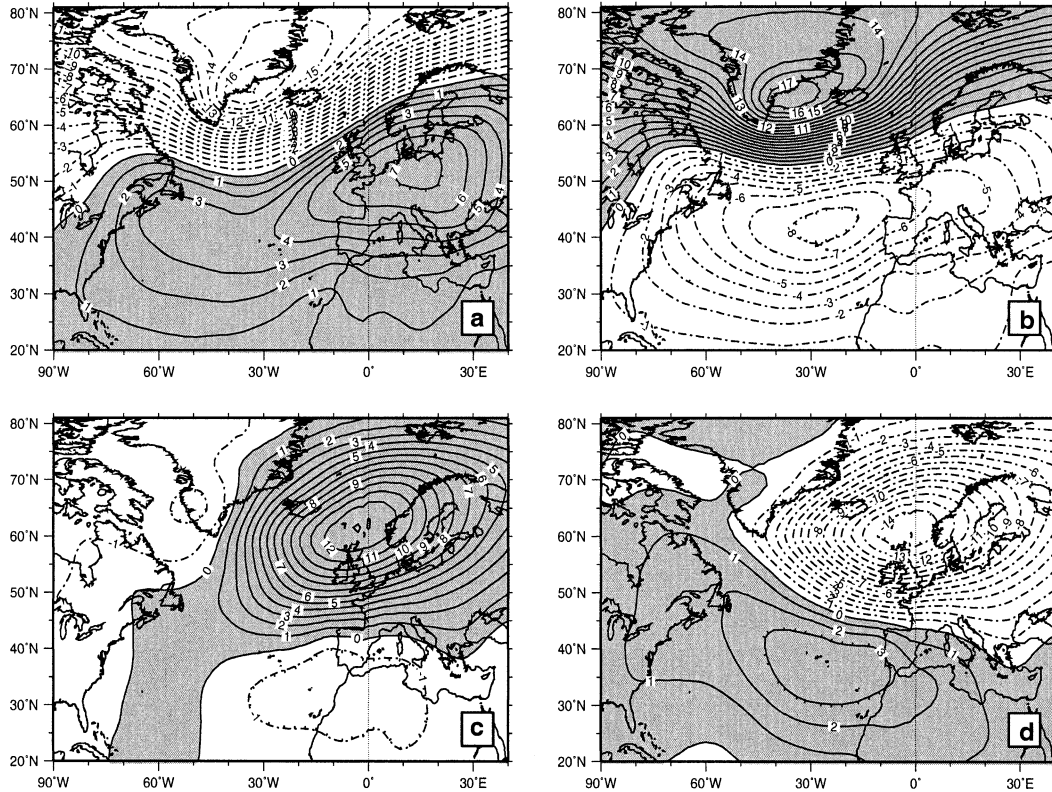


FIG. 7. Same as Fig. 6 but from NCEP reanalysis daily data. The percentage of occurrence are 21.5% and 24.5% for the NAO+ and NAO- weather regimes and 25.5% and 28.5% for the NE-high and NE-low regimes, respectively.

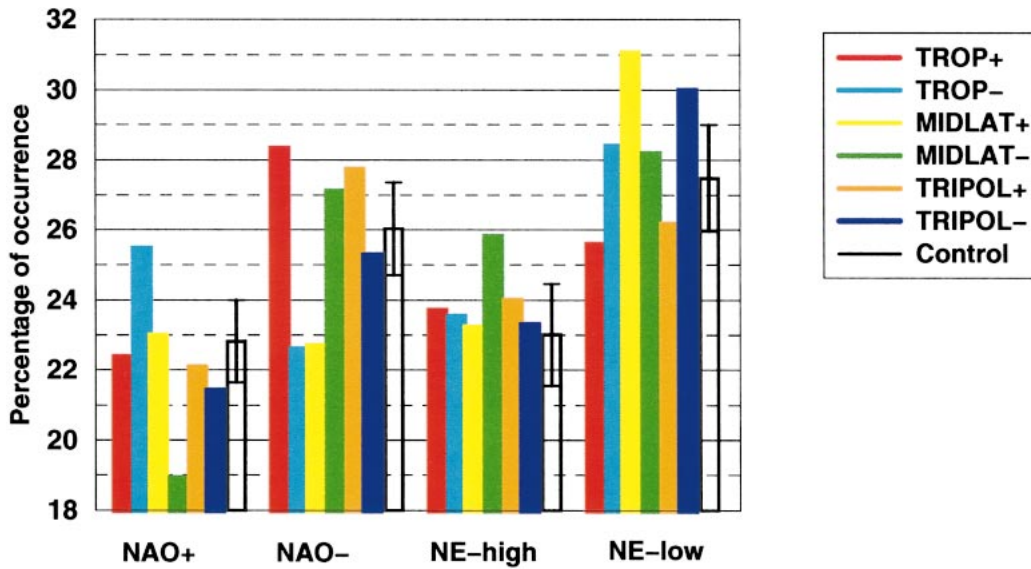


FIG. 8. Percentage of daily occurrences of the four regimes depending on experiments. As an estimate of the significance, the error bars correspond to the maximum dispersion of the decomposition estimated when the clustering is performed on anomaly maps with respect to individual experiments means.

et al. (2000) and represented in Fig. 8 by error bars. The latter quantify the maximum “within ensemble variability,” which can be interpreted as a conservative measure of random sampling variations. In practice, a new decomposition is done from anomaly maps based on individual experiment means and the error bar corresponds to the maximum difference of occurrence between experiments for a given regime in that configuration. The tropical ocean–atmosphere relationship is consistent with the observed link between the NAO phases and the tripole providing further evidence that its tropical branch forces the NAE variability in nature. The NE high is insensitive to tropical SST anomalies while the NE low is favored in cold versus warm conditions. The latter is consistent with the sign of the northernmost lobe of Rossby waves being excited from the western tropical Atlantic basin toward Scandinavia in response to North Atlantic tropical oceanic cooling (Terry and Cassou 2002).

Contrasting MIDLAT+ and MIDLAT− reveals an opposite picture. The NAO− (NAO+) regime is less frequent when high latitudes are warm (cold). Isolating the extratropical part of the observed pattern in an idealized context, the simulated ocean–atmosphere relationship would appear reversed compared to nature. If the atmospheric response of ARPEGE to midlatitude oceanic forcing is correct, this inverse simulated ocean–atmosphere link compared to reality suggests that the extratropical observed SST anomalies associated with the NAO are primarily a response to the atmospheric forcing. But according to the model, when taken separately, they may have a negative feedback as they would counteract the atmospheric pattern that initially created them. Note also that the NE high is favored when cold conditions (MIDLAT−) prevail at high latitude while the NE low is favored in MIDLAT+. This is consistent with Namias (1964) who suggested that enhanced blocking episodes occur when anomalous cold SST occurs off Newfoundland. Conclusions presented for MIDLAT, however, should be viewed with caution. Whereas signals are clear from a regime decomposition point of view, the mean atmospheric anomalies averaged over 30 yr for the MIDLAT experiments do not reveal any significant patterns, as in Sutton et al. (2001). Extratropical oceanic anomalies have also been shown to have a weak impact on the atmosphere (Kushnir et al. 2002).

Adding together tropical and extratropical oceanic forcing (TRIPOL) reveals some interesting features. Extratropical and tropical influences cancel each other in the model for the NAO+ regime, which then appears insensitive to the sign of the tripole. The tropical forcing still dominates the midlatitude one for the NAO− regime, but is reduced. This asymmetry between the two simulated NAO phase suggests that warm SST anomalies in the Tropics have more impact and might be related to the nonlinearities associated with convective activity and the Hadley cell. The overestimation of the

meridional circulation in ARPEGE calls again for caution in the interpretation of these results, which may be dependent on the simulation of the tropical mean state. As expected the NE high is insensitive to the tripole forcing while the tropical forcing on the NE low seems to be amplified by the presence of extratropical anomalies. This is consistent with Drévillon et al. (2003), which suggests the reinforcement of tropical impacts when a simple mixed-layer ocean model is added at midlatitudes. Similarly to our results, they found a stronger signal in the TRIPOL− case.

Finally, it is interesting to note that the weather regimes are not equally excited in the model. Intrinsically, NAO+ regimes seem to occur less frequently than NAO− ones as well as the NE high compared to the NE low. Similar results are obtained from NCEP daily data (Fig. 7). Referring to the occurrence of climate regimes, note also that NAO+ is less excited than NAO− during whatever period is considered. This asymmetry might be characteristic of the extratropical North Atlantic atmosphere and the model seems to be able to capture this dynamical property.

5. Summary and perspective

A cluster decomposition has been carried out on several observed SLP datasets over the last century for the North Atlantic–European domain. Four robust climate regimes have been extracted corresponding to the two phases of the NAO, a ridge regime and a west–east dipole between Greenland and Scandinavia. The asymmetrical perspective adopted in this study reveals a significant eastward shift of the NAO poles for the positive phase compared to the negative phase. The Azores high and the Icelandic low are displaced about 30° of longitude toward Europe, and this barotropic displacement is independent of the time period considered. It is therefore likely an intrinsic property of the NAO+ phase. This result affects the interpretation on the direct role of the greenhouse gases whose increased concentrations were hypothesized to play a role in the shift of Atlantic pressure poles in scenario experiments. According to our findings, the simulated displacement might be related to the preferred excitation of the NAO+ regimes in perturbed climate rather than to a drastic change of the atmospheric circulation.

The nonlinear approach also allows us to further document the nonstationarity of the North Atlantic–European variability in terms of amplitude and location. Decadal changes in SLP variance can be explained by the dominance of a given regime over a specific period. Within such a context, differences between the early part of the century and the last 50 years are related to the relative weight between NAO and RDG–GS regimes. Therefore, as the surface temperature and precipitation signatures associated with these regimes are quite different (van Loon and Madden 1983), it may not be enough, in a seasonal forecast perspective and

for impact studies, to predict only the NAO index. The latter may appear misleading when the NAO regimes are not dominant. It would be more accurate to assess the likelihood for the different regimes to occur.

The simultaneous oceanic surface anomalies related to the four regimes project, respectively, onto the two phases of the North Atlantic tripole mode, La Niña events, and warmer-than-average conditions in the Norwegian Sea. The asymmetrical perspective highlights that El Niño events might have less impact on the North Atlantic–European variability compared to La Niña events. The oceanic impact on the excitation of the North Atlantic–European weather regimes and their direct link to the climate regimes has been investigated using the ARPEGE model and a series of experiments perturbed by SST anomalies at specific locations. We have shown that model results tend to confirm the active role of tropical North Atlantic oceanic conditions to explain the North Atlantic–European observed interannual variability. Analyses on weather regimes reveal that the oceanic forcing affects the excitation mechanism of high-frequency atmospheric modes to favor one sign over the other. Climate regimes can be thus interpreted as the time-averaged signature of this forcing. The NAO+ shift of the Azores high is well captured in the model as well as the uneven frequency of occurrence of the regimes. Extratropical SST anomalies produce a significant atmospheric response in the model but one that is opposite to the observed ocean–atmosphere relationship. This suggests that the extratropical oceanic conditions might counteract the tropical impact. Our results thus illustrate that tropical and extratropical contribution are nonadditive and very nonlinear. It is therefore dangerous to consider them separately as they are intrinsically linked.

Acknowledgments. We thank R. Madden and R. Sutton for stimulating discussions. The main author is grateful to A. Phillips for help accessing and plotting the data with the NCL software. This work is supported by the European Community via the 5th framework program PREDICATE project under Contract EVK2-CT-1999-00020 and by NOAA under Grant NA06GP0394.

REFERENCES

- Alhamed, A., S. Lakshminarayanan, and D. J. Stensrud, 2002: Cluster analysis of multimodel ensemble data from SAMEX. *Mon. Wea. Rev.*, **130**, 226–256.
- Allen, M., and L. Smith, 1997: Optimal filtering in singular spectrum analysis. *Phys. Lett.*, **234**, 419–428.
- Anderberg, M. R., 1973: *Cluster Analysis for Applications*. Academic Press, 359 pp.
- Barnston, A. G., and R. E. Livezey, 1987: Classification, seasonality and persistence of low frequency atmospheric circulation patterns. *Mon. Wea. Rev.*, **115**, 1083–1126.
- Blackmon, M. L., Y. H. Lee, and J. M. Wallace, 1984: Horizontal structure of 500 mb height fluctuations with long, intermediate and short time scales. *J. Atmos. Sci.*, **41**, 961–979.
- Cassou, C., 2001: Rôle de l’océan dans la variabilité basse fréquence de l’atmosphère sur la région Nord Atlantique-Europe. Ph.D. dissertation, University of Toulouse, 280 pp.
- , and L. Terray, 2001: Oceanic forcing of the wintertime low frequency atmospheric variability in the North Atlantic European sector: A study with the ARPEGE model. *J. Climate*, **14**, 4266–4291.
- Chen, W., 1982: Fluctuations in the Northern Hemisphere 700 mb height field associated with the Southern Oscillation. *Mon. Wea. Rev.*, **110**, 808–823.
- Cheng, X., and J. M. Wallace, 1993: Cluster analysis of the Northern Hemisphere wintertime 500-hPa height field: Spatial patterns. *J. Atmos. Sci.*, **50**, 2674–2696.
- Corti, S., F. Molteni, and T. N. Palmer, 1999: Signature of recent climate changes in frequencies of natural circulation regimes. *Nature*, **398**, 799–802.
- Davies, R. E., B. P. Hayden, D. A. Gay, W. L. Phillips, and G. V. Jones, 1997: The North Atlantic subtropical anticyclone. *J. Climate*, **10**, 728–744.
- Déqué, M., C. Dreveton, A. Braun, and D. Cariolle, 1994: The climate version of ARPEGE/IFS: A contribution to the French community climate modelling. *Climate Dyn.*, **10**, 249–266.
- Drévillon, M., 2002: Interaction océan–atmosphère à l’échelle saisonnière sur la région Atlantique Nord-Europe: Rôle des routes dépressionnaires et mécanismes associés sur la variabilité climatique. Ph.D. dissertation, University of Toulouse, 179 pp.
- , C. Cassou, and L. Terray, 2003: Model study of the wintertime atmospheric response to fall tropical Atlantic SST anomalies. *Quart. J. Roy. Meteor. Soc.*, **129**, 2591–2611.
- Feldstein, S. B., 2000: The timescale, power spectra and climate noise properties of teleconnection patterns. *J. Climate*, **13**, 4430–4440.
- Gillett, N., H. F. Graf, and T. J. Osborn, 2003: Climate change and the North Atlantic Oscillation. *North Atlantic Oscillation: Climate Significance and Environmental Impact*, Geophys. Monogr., Vol. 134, Amer. Geophys. Union, 193–209.
- Halpert, M., and C. Ropelewski, 1992: Surface temperature patterns associated with the Southern Oscillation. *J. Climate*, **5**, 577–593.
- Hannachi, A., 2001: Toward a nonlinear identification of the atmospheric response to ENSO. *J. Climate*, **14**, 2138–2149.
- Hilmer, M., and T. Jung, 2000: Evidence for a recent change in the link between the North Atlantic Oscillation and Arctic sea ice export. *Geophys. Res. Lett.*, **27**, 989–992.
- Hoskins, B., I. James, and G. White, 1983: The shape, propagation and mean flow interaction of large scale weather systems. *J. Atmos. Sci.*, **40**, 1595–1612.
- Hurrell, J. W., 1995: Decadal trends in the North Atlantic Oscillation and relationships to regional temperature and precipitation. *Science*, **269**, 676–679.
- , and H. van Loon, 1997: Decadal variations associated with the North Atlantic Oscillation. *Climate Change*, **36**, 301–326.
- Kalnay, E., and Coauthors, 1996: The NCEP/NCAR 40-Year Reanalysis Project. *Bull. Amer. Meteor. Soc.*, **77**, 437–471.
- Kimoto, M., and M. Ghill, 1993: Multiple flow regimes in the Northern Hemisphere winter. Part I: Methodology and hemispheric regimes. *J. Atmos. Sci.*, **50**, 2625–2643.
- Kushnir, Y., W. A. Robinson, I. Bladé, N. M. J. Hall, S. Peng, and R. T. Sutton, 2002: Atmospheric GCM response to extratropical SST anomalies: Synthesis and evaluation. *J. Climate*, **15**, 2233–2256.
- Lorenz, E. N., 1963: Deterministic nonperiodic flow. *J. Atmos. Sci.*, **20**, 130–148.
- Martineu, C., J. Caneill, and R. Sadourny, 1999: Potential predictability of European winters from the analysis of seasonal simulations with an AGCM. *J. Climate*, **12**, 3033–3061.
- Michelangeli, P., R. Vautard, and B. Legras, 1995: Weather regime recurrence and quasi stationarity. *J. Atmos. Sci.*, **52**, 1237–1256.
- Monahan, A. H., L. Pandolfo, and J. C. Fyfe, 2001: The preferred structure of variability of the Northern Hemisphere atmospheric circulation. *Geophys. Res. Lett.*, **28**, 1019–1022.
- Namias, J., 1964: Seasonal persistence and recurrence of European blocking during 1958–1960. *Tellus*, **16**, 394–407.

- Palmer, T., 1999: A non-linear dynamical perspective on climate prediction. *J. Climate*, **12**, 575–591.
- Peng, S., and J. Fyfe, 1996: The coupled patterns between sea level pressure and sea surface temperature in the midlatitude North Atlantic. *J. Climate*, **9**, 1824–1839.
- , and J. Whitaker, 1999: Mechanisms determining the atmospheric response to midlatitude SST anomalies. *J. Climate*, **12**, 1393–1408.
- Reynolds, R. W., and T. M. Smith, 1995: A high resolution global sea surface temperature climatology. *J. Climate*, **8**, 1571–1583.
- Robertson, A. W., C. Mechoso, and Y. Kim, 2000: The influence of Atlantic sea surface temperature anomalies on the North Atlantic Oscillation. *J. Climate*, **13**, 122–138.
- Sutton, R. T., W. A. Norton, and S. P. Jewson, 2001: The North Atlantic Oscillation—What role for the ocean? *Atmos. Sci. Lett.*, **1**, 89–100.
- Terray, L., and C. Cassou, 2002: Tropical Atlantic sea surface temperature forcing of the quasi-decadal climate variability over the North Atlantic–Europe region. *J. Climate*, **15**, 3170–3187.
- Thompson, D., and J. M. Wallace, 1998: The Arctic Oscillation signature in wintertime geopotential heights and temperature fields. *Geophys. Res. Lett.*, **25**, 1297–1300.
- Trenberth, K. E., and D. A. Paolino, 1980: The Northern Hemisphere sea level pressure dataset: Trends, errors and discontinuity. *Mon. Wea. Rev.*, **108**, 855–872.
- Ulbrich, U., and M. Christoph, 1999: A shift of the NAO and increasing storm track activity over Europe due to anthropogenic greenhouse gas forcing. *Climate Dyn.*, **15**, 551–559.
- van Loon, H., and R. A. Madden, 1983: Interannual variations of mean monthly sea level pressure in January. *J. Climate Appl. Meteor.*, **22**, 687–692.
- Vautard, R., 1990: Multiple weather regimes over the North Atlantic: Analysis of precursors and successors. *Mon. Wea. Rev.*, **118**, 2056–2081.
- Venzke, S., M. R. Allen, R. T. Sutton, and D. P. Rowell, 1999: The atmospheric response over the North Atlantic to decadal changes in sea surface temperature. *J. Climate*, **12**, 2562–2584.
- Wallace, J. M., and D. Gutzler, 1981: Teleconnections in the geopotential fields during the Northern Hemisphere winter. *Mon. Wea. Rev.*, **109**, 784–812.
- Walsh, J. E., A. S. Phillips, D. H. Portis, and W. L. Chapman, 2001: Extreme cold outbreaks in the United States and Europe, 1948–99. *J. Climate*, **14**, 2642–2658.
- Ward, J., 1963: Hierarchical grouping to optimize an objective function. *J. Amer. Stat. Assoc.*, **58**, 236–244.
- Watanabe, M., and M. Kimoto, 2000: Atmosphere–ocean thermal coupling in the North Atlantic: A positive feedback. *Quart. J. Roy. Meteor. Soc.*, **126**, 3343–3369.
- Yu, X., and M. J. McPhaden, 1999: Dynamical analysis of seasonal and interannual variability in the equatorial Pacific. *J. Phys. Oceanogr.*, **29**, 2350–2369.